AN APPROACH GUIDANCE SYSTEM FOR SIDE-FIRING TACTICAL AIRCRAFT

by

LT COL BRADFORD W. PARKINSON
MAJOR EDWARD J. BAUMAN
CAPTAIN JACK C. HENRY

TECHNICAL REPORT 70-4
OCTOBER 1970

UNITED STATES AIR FORCE ACADEMY
COLORADO 80840

AN APPROACH GUIDANCE SYSTEM FOR SIDE-FIRING TACTICAL AIRCRAFT

by

Lt Colonel Bradford W. Parkinson
Major Edward J. Bauman
Captain Jack C. Henry

UNITED STATES AIR FORCE ACADEMY

TECHNICAL REPORT 70-4

OCTOBER 1970

Editor: Major Jimmie L. Jay, USAF

The research reported in this document was made possible in part by support extended to the faculty of the United States Air Force Academy by the Air Force Systems Command.

Additional copies of this document may be obtained by writing to the Director of Faculty Research, United States Air Force Academy, Colorado 80840

This Technical Report is presented as a competent treatment of the subject, worthy of publication. The United States Air Force Academy vouches for the quality of the research, without necessarily endorsing the opinions and conclusions of the authors.

TABLE OF CONTENTS

ABSTRACT

The present approach guidance scheme is one of controlling the aircraft's velocity vector; however, this scheme has two major disadvantages:

(1) it's a difficult flying task for the pilot, and

(2) when the aircraft arrives tangent to the circular path, a violent maneuver is usually required to achieve the proper bank angle to stay on the desired circular path.

An improved method for controlling the side firing AC-130 and AC-119 into circular attack geometry eliminates these disadvantages. Furthermore, with this improved system the bank angle rates never exceed 3 or 4 degrees per second. This control scheme was simulated on the analog computer and the results are presented graphically. The simulation showed that the bank angle, command-control scheme is effective for distances out to five circular orbit radii from the target and is effective for all aircraft headings (with one exception which is discussed in a stability study in the appendix). The initial test flight showed that the bank angle control scheme behaved very well, and its overall performance was near that predicted. Relatively minor modifications can incorporate this control scheme into existing analog computers on board the aircraft.

LIST OF FIGURES

LIST OF SYMBOLS

Symbol	Description
Δ	radial error (See Figure 2, page 3)
L	tangential error (See Figure 2, page 3)
g	acceleration of gravity
φ	bank angle
K_1	constant Δ multiplier used in control law
K_2	constant L multiplier used in control law
R	circular attack radius
V	velocity of aircraft
x_1	Δ normalized by R
x_2	L normalized by R
φ_a	actual aircraft bank angle
v_a	voltage at point "A" in aircraft analog computer (See Figure 11, page 21)
S_1, S_2, S_3	amplifier gains in the aircraft analog computer
R_f, R_φ	resistors in the aircraft analog computer
$\underline{D}$	vector distance from aircraft to target
$\underline{j}$	unit vector along aircraft's velocity vector
$\underline{i}$	unit vector 90° to the left of $\underline{j}$
$\underline{k}$	unit vector perpendicular to plane containing $\underline{i}$ and $\underline{j}$
$\underline{\omega}$	angular rotation of aircraft's velocity vector
m	mass of aircraft
F	local horizontal force on aircraft
r	radius of turn of aircraft
c_1	K_1 normalized by R
c_2	K_2 normalized by R
ζ	damping ratio

Symbol	Description
ω_n	natural frequency
z_λ	λ magnitude scaled for analog computer simulation
z_ρ	L magnitude scaled for analog computer simulation
x,y	ground track coordinates
$\dot{(\ )}$	derivitive of (L) with respect to time
$\underline{(\ )}$	vector quantity
$\Delta(\ )$	incremental change of ( )
$(\ )_n$	normalizing constant for ( )
λ	eigenvalue

I. Background

The Air Force Academy's Department of Astronautics has been involved in a continuing program of technical consultation for the Deputy for Limited War, WPAFB, Ohio. As part of this program we were asked to look at the current approach guidance used in the side firing AC-130 and AC-119 to see if any simple improvements could be made. (Approach guidance when used in this report refers to the guidance of an aircraft into a circular attack geometry.)

The present approach guidance scheme is one of controlling the aircraft's velocity vector; however, the present scheme seems inadequate. We propose a replacement for the present system: a bank angle approach guidance scheme. The main topics of this report are: the derivation of this scheme, its Analog simulation, and the method of implementation.

II. The Need for Improvement

The present approach guidance system for side-firing tactical aircraft is designed to have the pilot fly the aircraft toward a fixed offset distance from the final circular flight path. Near this offset point the pilot is given information on how far he is off the circular path; he then tries to drive these distances to zero.

The problem of attempting to zero out distances by controlling the aircraft's velocity vector is a difficult task. In this case, it is compounded by the fact that the coordinate distances to a circular path change with the heading of the velocity vector and with the position of the aircraft. Finally, the greatest difficulty is getting on the circular path with the proper bank angle to maintain that circular path. Often the aircraft arrived on the path flying straight and level - or banked in the wrong direction. This caused violent maneuvers when the pilot attempted to correct to the proper bank angle to maintain the aircraft on the desired circular path.

One solution is to use the computer to translate distance information into a bank angle command rather than null distance information. When the distances go to zero, the commanded angle would be the one which puts the aircraft on the circular flight path. [The system of presenting bank angle information rather than distance information has recently been adopted for instrument landing systems (ILS) and has proved very effective.]

Present System

Figure 1 shows the typical ground track of the aircraft flying toward the circular path. At position 1 the aircraft is flying straight toward an offset point as shown. As the aircraft approaches the circle, it turns to fly tangent (position 2). With the present system there is no guarantee that the aircraft will be banked properly at position 2 to continue in the circular path. This is true since the approach guidance system only brings the aircraft tangent to the circular path, and another guidance system is then switched on to keep the aircraft on the circular path.

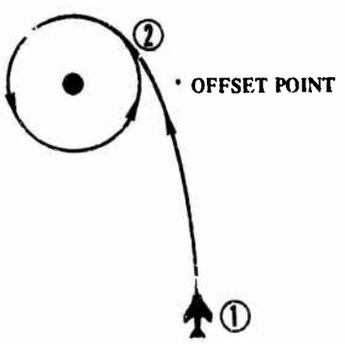

Figure 1: Aircraft Ground Track

The proposed approach system not only brings the aircraft tangent to the circle but ensures that the aircraft is in the proper bank to maintain that circle. We call this new system bank-angle approach guidance; the next section contains a discussion of the theory involved.

III. Bank Angle Approach Guidance System Theory

Kinematic and Approach Guidance Equations - The aircraft is considered a point mass flying in a horizontal plane, so that lift always balances weight; the vertical dimension is ignored. Figure 2 shows a diagram of the two dimensional geometry. The coordinate Δ is measured along a line from the target and drawn perpendicular to the aircraft's instantaneous flight path. The coordinate L is measured along the aircraft flight path. $\underline{V}$ is the velocity vector of the aircraft and $\underline{\omega}$ is

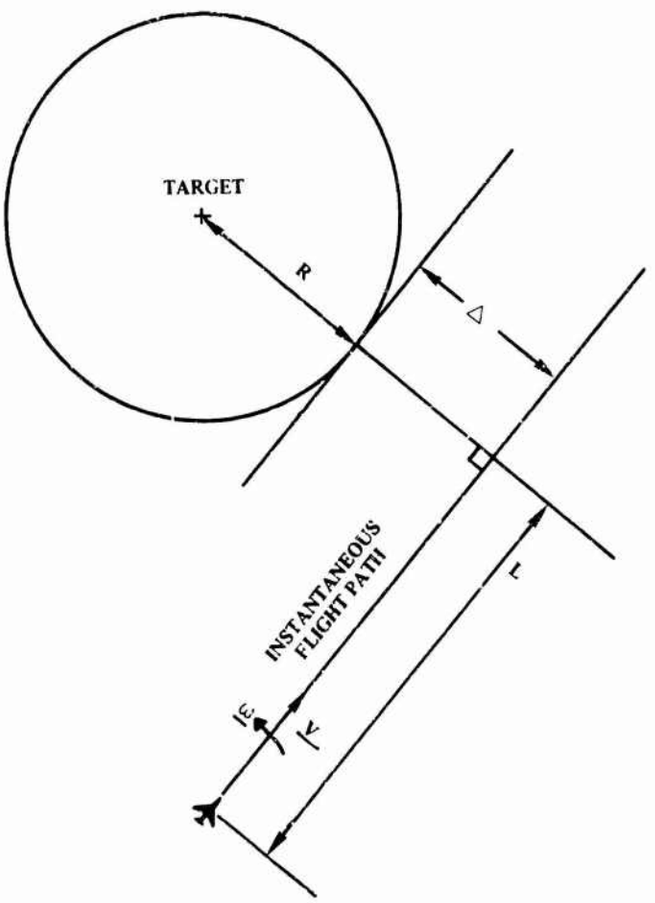

Figure 2: Geometry Defining Radial Error (Δ) and Tangential Error (L)

its angular rotation rate. The magnitude of $\underline{V}$ is considered constant. R is the magnitude of the circle radius. The equations for $\dot{\Delta} = \frac{d\Delta}{dt}$, $\dot{L}$ $\frac{dL}{dt}$ are given below and are derived in Appendix A.

$$\dot{\Delta} = -\omega L \qquad (1)$$

$$\dot{L} = -V + (R + \Delta)\omega \qquad (2)$$

where for any coordinated turn

$$\omega = \frac{g \tan \phi}{V} \qquad (3)$$

g = acceleration of gravity, and

ϕ = bank angle

$$\text{Let } \phi = \phi_o + \delta\phi \qquad (4)$$

where ϕ_o = .524 radians (30^o) is the desired bank angle to fly the circular path. We shall <u>choose</u> a linear feedback guidance scheme such that:

$$\delta\phi = K_1\Delta + K_2L \qquad (5)$$

where K_1 and K_2 are constants. Finally substituting (3), (4) and (5) into (1) and (2) we have:

$$\dot{\Delta} = -\frac{L}{V} g \tan (.524 + K_1\Delta + K_2L) \qquad (6)$$

$$\dot{L} = -V + \frac{(R+\Delta)}{V} g \tan (.524 + K_1\Delta + K_2L) \qquad (7)$$

Equations (6) and (7) have an equilibrium point at

$$L = \Delta = 0$$

and this point is stable if

$$K_1 > 0 \text{ and } K_2 < 0 \quad \text{(see Appendix B).} \qquad (8)$$

Therefore, we expect our guidance system to operate well in the neighborhood of the circular path.

We made an analog simulation of equations (6) and (7) to ensure that the guidance system would continue to operate effectively when far from the circular path. This simulation is described in the next section.

IV. Analog Simulation

To facilitate programming on the analog computer, equations (6) and (7) were normalized by dividing by R:

$$\frac{\dot{\Delta}}{R} = -\frac{g}{V}\left(\frac{L}{R}\right) \tan (.524 + \delta\varphi)$$

$$\frac{\dot{L}}{R} = -\frac{V}{R} + \left(1+\frac{\Delta}{R}\right) \frac{g}{V} \tan (.524 + \delta\varphi)$$

and

$$\delta\varphi = K_1 R\left(\frac{\Delta}{R}\right) + K_2 R\left(\frac{L}{R}\right) .$$

Defining $x_1 = \frac{\Delta}{R}$ and $x_2 = \frac{L}{R}$ we have:

$$\dot{x}_1 = -\frac{g}{V} x_2 \tan (.524 + \delta\varphi) \qquad (9)$$

$$\dot{x}_2 = -\frac{V}{R} + (1+x_1) \frac{g}{V} \tan (.524 + \delta\varphi) \qquad (10)$$

...id

$$\ddot{\varphi} = K_1 Rx_1 + K_2 Rx_2 \qquad (11)$$

The equations were then magnitude and time scaled to prevent computer voltage overloads and to speed the solution time. The details of the simulation are given in Appendix C where V = 300 fps, and the corresponding R = [illegible] ft.

Some added features of the system and simulation are:

(a) The actual $\ddot{\varphi}$ is generated from Δ and a limited L:

$\ddot{\varphi} = K_1\Delta + K_2 L'$ where the characteristic of L' is as shown in Figure 3.

When L is limited, i.e. $|L| > 2000$ ft., then φ in radians is given by

$$\ddot{\varphi} = .524 + K_1\Delta + 2000K_2;\ K_1 > 0 \text{ and } K_2 < 0 . \qquad (12)$$

Under these conditions, the only stable solution of (6) and (7) is $\ddot{\varphi} = 0$ because if $\varphi > 0$, then from (6) $\dot{\Delta} < 0$ and from (12), φ will decrease. Likewise if $\ddot{\varphi} < 0$, then $\Delta > 0$ and from (12) φ will

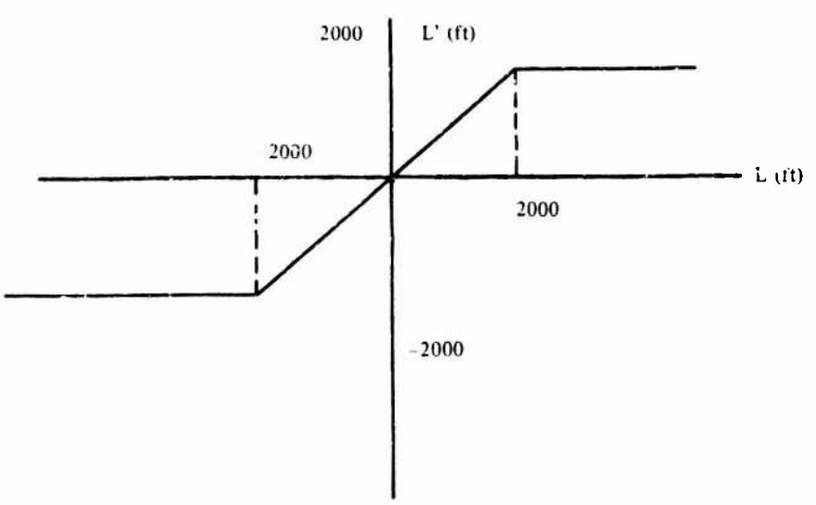

Figure 3: L Limiter

increase. Now with $\varphi = 0$, (6) and (7) become $\dot{\Delta} = 0$ and $\dot{L} = -V$. The aircraft flys in a straight line toward a Δ offset point as shown in Figure 1. The value of Δ can be calculated from (12) with $\varphi = 0$,

$$\Delta \text{ offset} = \frac{.524 + 2000K_2}{K_1} \qquad (13)$$

(b) A simple first order time lag of 2.0 sec was introduced in the simulation to approximate the dynamics of the pilot and aircraft in executing a bank command. This time lag is given by

$$\dot{\varphi}_a = 0.5\ (\varphi - \varphi_a) \qquad (14)$$

Where φ_a is the actual aircraft bank angle. Also, the commanded bank angle was limited to $\pm 40^{\circ}$ in the simulation.

(c) The simulation included a programmed ground track showing the aircraft's position.

Figure 4 illustrates a functional block diagram of the simulation indicating the features previously described.

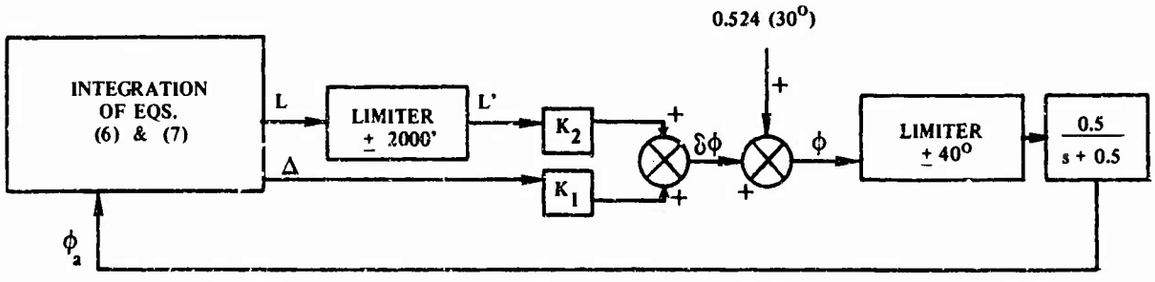

Figure 4: Functional Block Diagram of the Analog Computer Simulation

V. Results and Conclusions

Figures 5 through 10 show the results of the simulation and illustrate the following:

(a) Aircraft ground track

(b) Bank angle, ϕ_a

(c) In some cases, bank angle rate.

As shown in Section VI, the values $K_1 = 3.5 \times 10^{-4}$ and $K_2 = -3.5 \times 10^{-4}$ gave satisfactory responses and were easily implemented.

From the stability analysis, Appendix B, the linearized system, which holds near the circular flight path, shows that as a second order approximation this system has a natural frequency of about .14 rad/sec and a damping ratio of about 0.9. Furthermore, the approach behavior far from the circular path is essentially a straight line heading to a Δ offset point calculated from (13) as 500 feet. Figures 5 through 10 show about the same Δ offset; that is, Δ/R approximately equal to 0.1.

The significant feature of this system, as shown in Figures 5 and 7, is that the final approach bank angle rates are never more than 3 or 4 deg/sec. This is well within the capabilities of the aircraft. Larger bank rates are sometimes experienced during the initial maneuver to turn onto the straight line flight path, but are not excessive. If the pilot cannot follow the commanded bank, he will simply fly a slightly different path, but, essentially, he will arrive on the circle at the same point with about the same final bank rates.

Bank angle acceleration is not greater than about 1 deg/sec^2, again well within aircraft capabilities. In all cases, the final bank angle of 20^o is achieved when the aircraft arrives at the circular flight path.

A time lag of 5 seconds rather than 2 seconds was also used in the simulation. This simulated longer delays for the pilot and aircraft to respond to the commanded bank angle. The results showed that a slightly larger flight path was flown and that there tended to be an overshoot of

the final 30^{o} bank angle because the angle became larger than 30^{o} before settling back to 30^{o}. However, the system still behaved satisfactorily by bringing the aircraft onto the circular path.

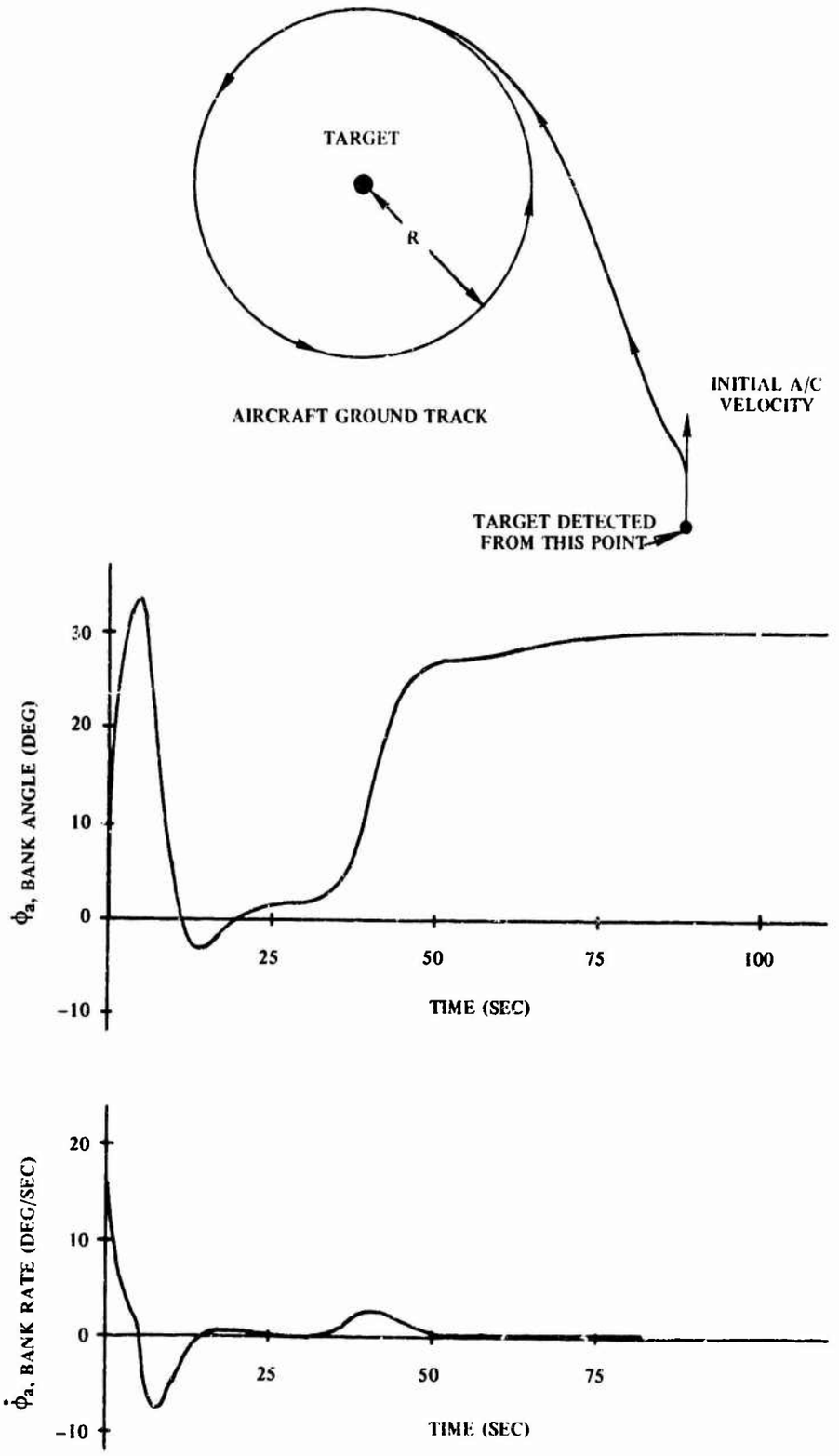

Figure 5: Ground Track, Bank, and Bank Rate

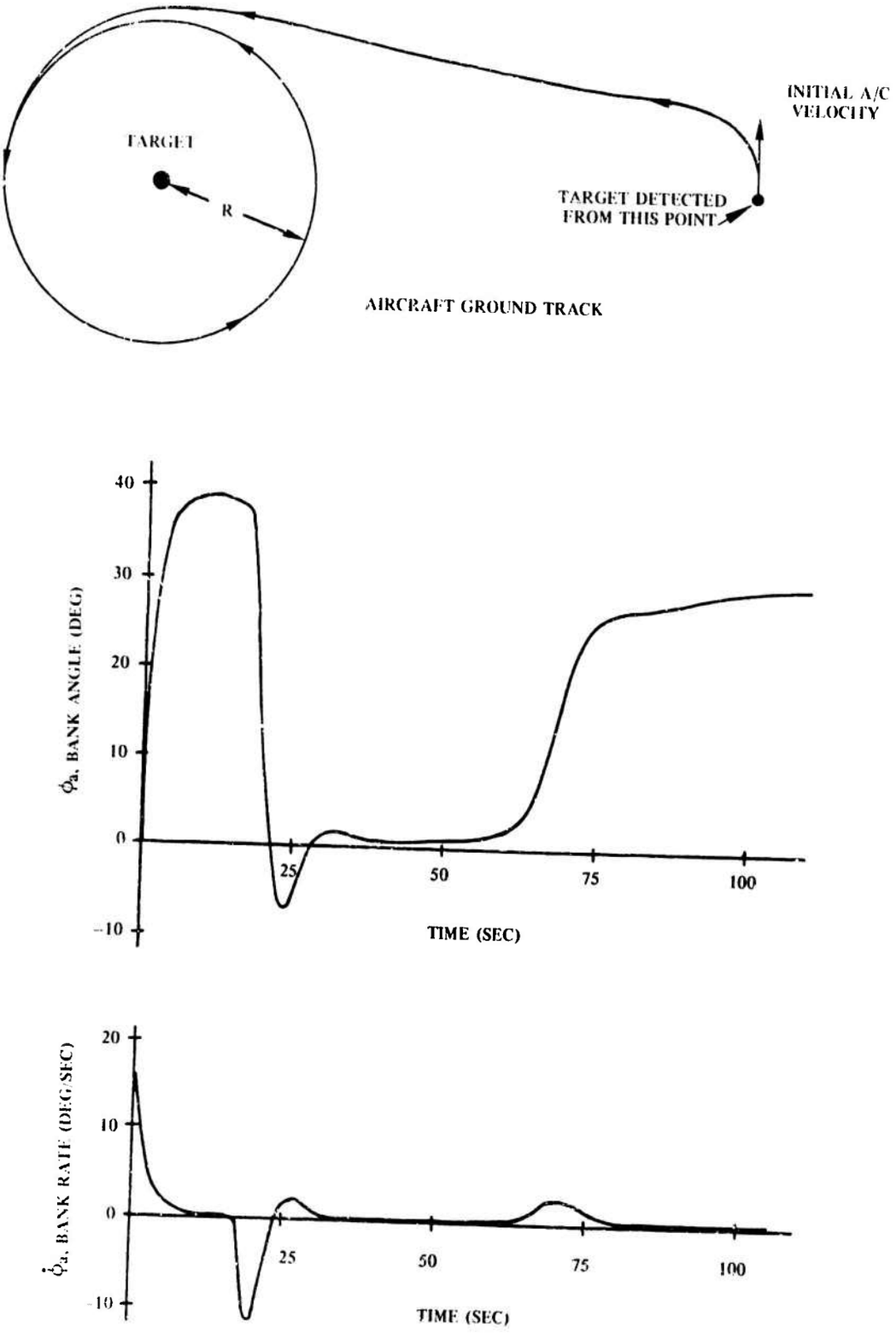

Figure 6: Ground Track, Bank, and Bank Rate

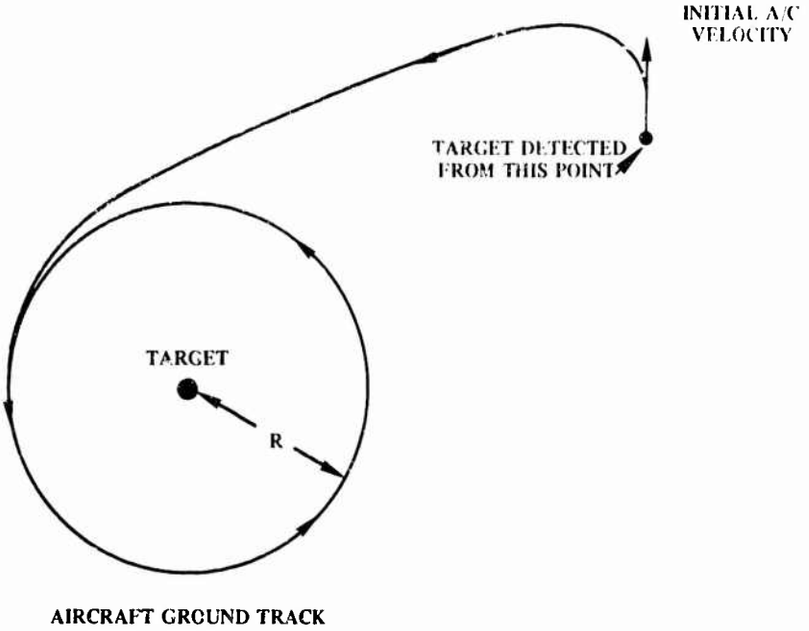

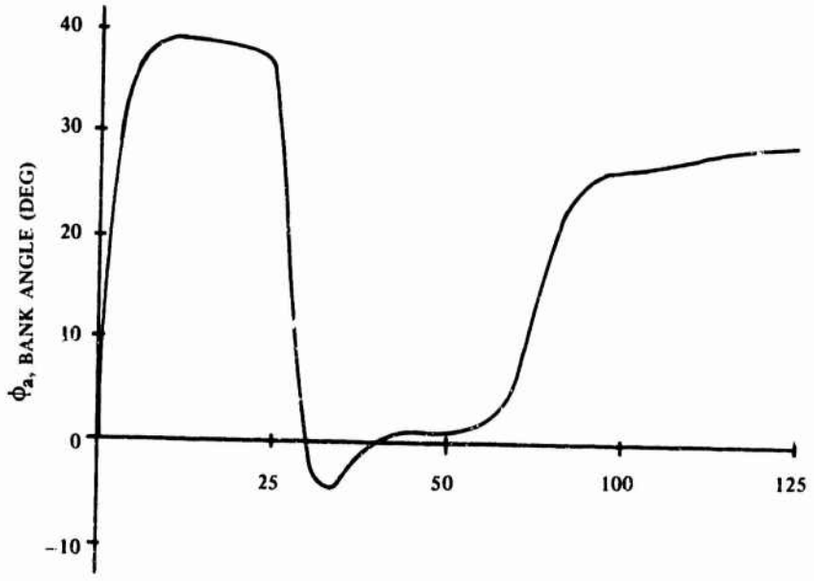

Figure 7: Ground Track and Bank

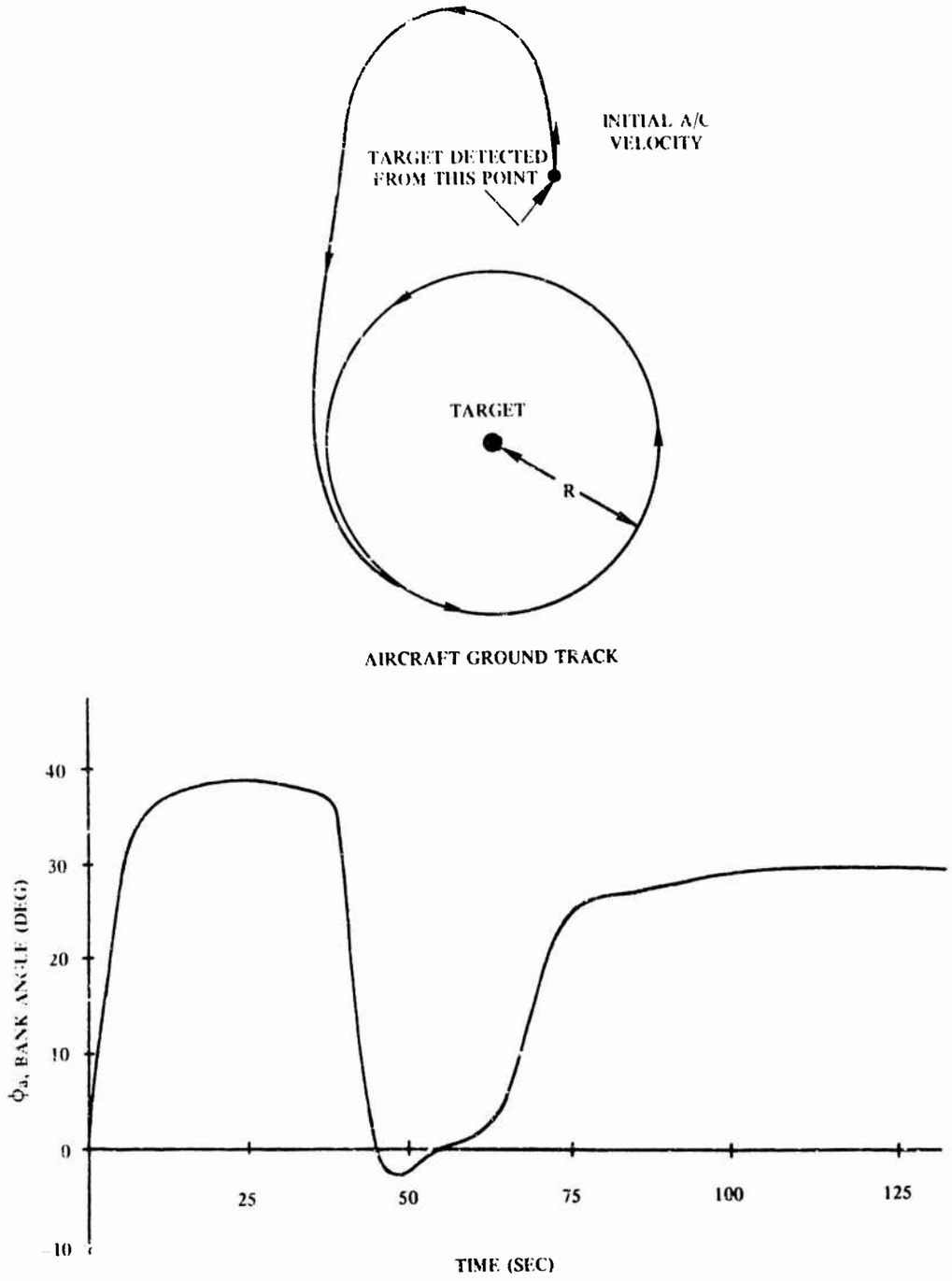

Figure 8: Ground Track and Bank

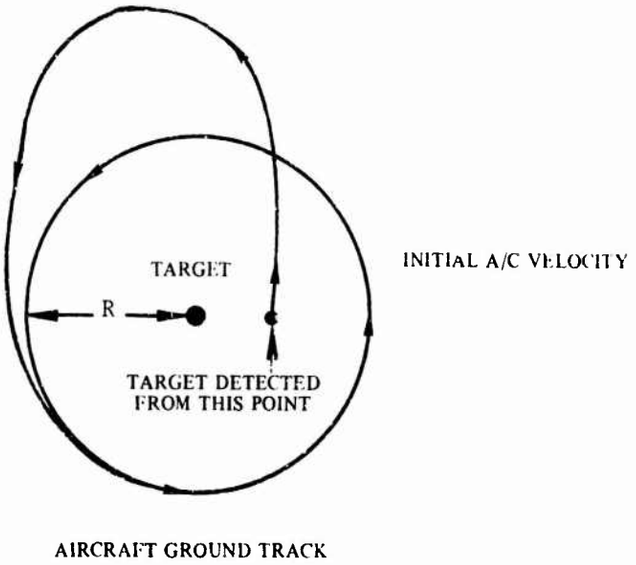

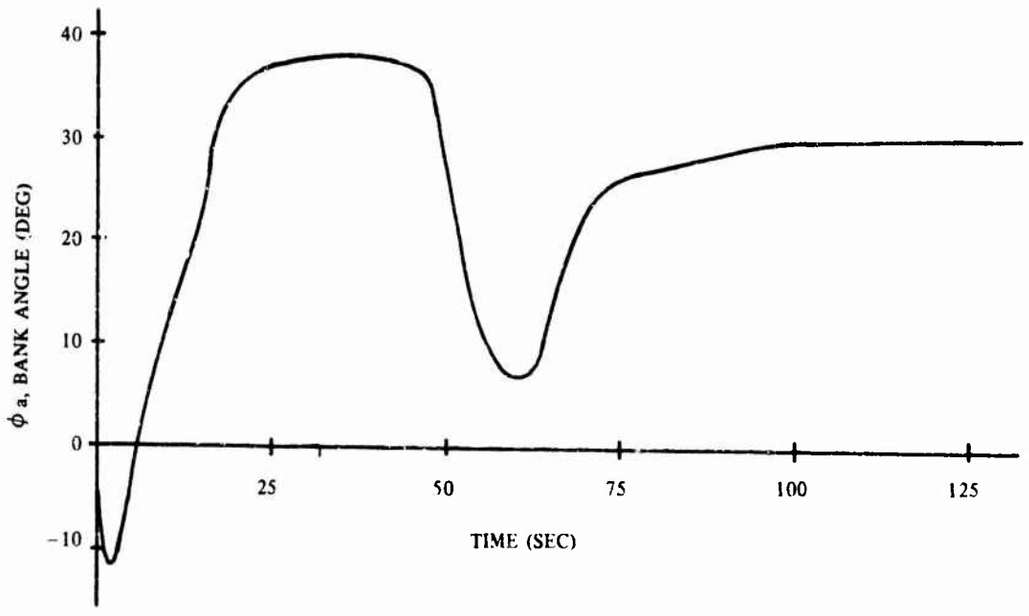

Figure 9: Ground Track and Bank

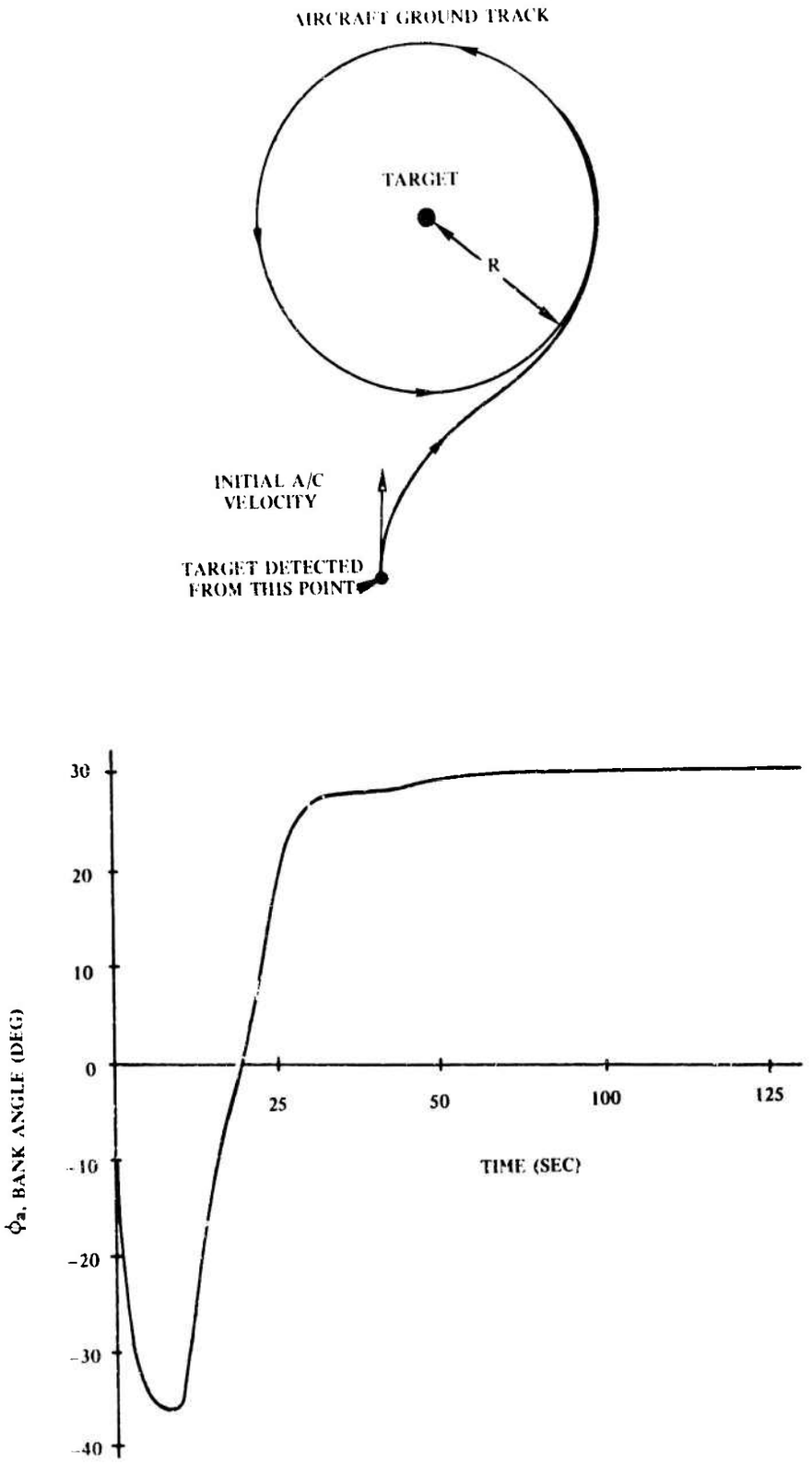

Figure 10: Ground Track and Bank

VI. Implementation of the New System

The system has been implemented in the analog computer as shown in Figure 11. The added components are shown by an asterisk.

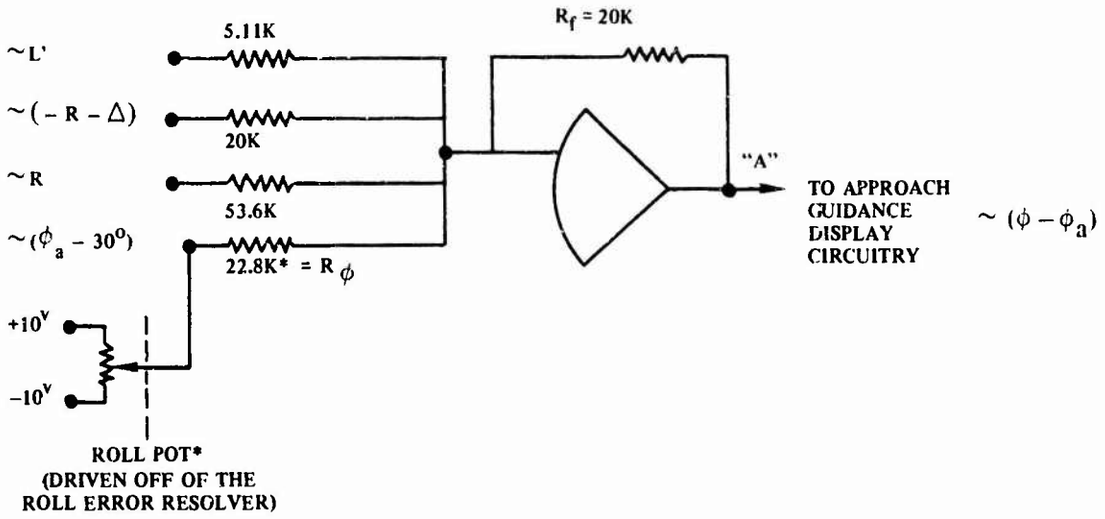

Figure 11: Analog Computer Diagram Showing Added Components

NOTE:

(1) ~ means proportional to

(2) At point "A", 1 ft of distance corresponds to 1 mv.

(3) At point "A", 1 deg corresponds to 50 mv.

(4) * denotes added components.

(5) Roll and bank are synonymous.

The following calculation gives the value of the 22.8K resistor. The voltage at "A", v_A, is given by:

$$v_A = S_1(.25 - \phi_a) + S_2(\quad) - S_3 L \text{ volts} \qquad (15)$$

where S_1 measured in v/rad is to be determined, and $S_2 = S_3 = .001$ v/ft.

[Note: $\phi^{\circ} = .25$]

From ( ) and ( )

$$\phi = .25 + (\quad) \times 10^{-4}(\quad - L) \text{ rad.} \qquad (16)$$

Dividing (15) by S_1, we obtain the same form as (16)

$$\frac{v_A}{S_1} = .25 - \phi_a + \frac{.001}{S_1}(\quad - L) \text{ rad.} \qquad (17)$$

Comparing (16) and (17) we see that

$$(\quad) \times 10^{-4} = \frac{.001}{S_1}$$

or $S_1 = 2.56$ v/rad $= 0$ mv/deg.

Now the sensitivity of the roll potentiometer is just 20 volts/350 deg = $\quad$ mv/deg. Therefore, the sensitivity must be <u>reduced</u> going through the amplifier; if R_ϕ is the value of the roll potentiometer resistor and $R_f = 20K$ is the value of the feedback resistor,

then

$$\text{Amp Gain} = \frac{R_f}{R_\phi} = \frac{20}{\quad} \text{ or } R_\phi = 22.8K.$$

Finally, the pilot display is similar to the one shown in Figure 12. The value of L is fed to the horizontal bar. The value of $\phi - \phi_a$ is fed to the vertical bar. When $\phi - \phi_a = 0$, the vertical needle is centered, and the pilot is flying the commanded bank angle. When L=0, the horizontal needle is centered, and the aircraft is flying with one wing pointed along the azimuth of the target. When both $\phi - \phi_a$ and L <u>remain</u> zero, the aircraft is flying the desired circular flight path.

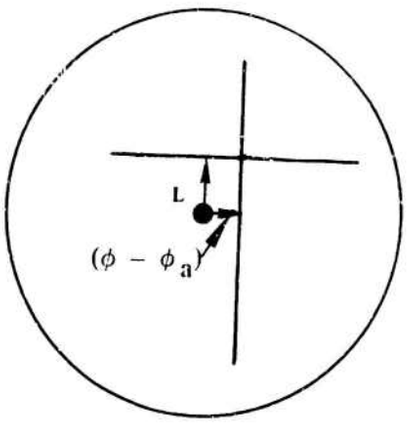

Figure 12: Pilot Display of L and $\phi - \phi_a$

APPENDIX A

Derivation of $\dot{\Delta}$ and $\dot{L}$

Figure 13 shows the coordinate system of L and Δ.

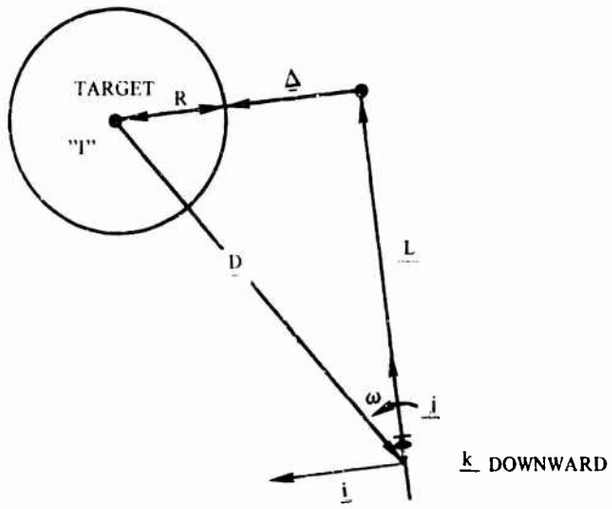

Figure 13: Coordinate System Defined

The rotating coordinate system is defined by the unit vectors $\underline{i}$, $\underline{j}$, and $\underline{k}$. The coordinate system rotates with the aircraft velocity vector: $\underline{j}$ along the vector and $\underline{i}$ 90° to the left of the vector. The rotation of the velocity vector is $\underline{\omega} = -\omega\underline{k}$; thus $\underline{i}$ and $\underline{j}$ stay in the horizontal plane since $\underline{k}$ is perpendicular to the horizontal plane.

$$-\underline{D} = (R+\Delta)\ \underline{i} = L\underline{j} \qquad (A\text{-}1)$$

Differentiating D with respect to time in an assumed inertial (target) coordinate frame, "I".

$$-\dot{\underline{D}}\Big|_I = (\dot{R}+\dot{\Lambda})\underline{i} + (R+\Lambda)\dot{\underline{i}} + \dot{L}\underline{j} + L\dot{\underline{j}} \qquad \text{(A-2)}$$

but $\underline{D}\Big|_I$ = velocity of the aircraft = $V\underline{j}$, $\dot{R}=0$, $\dot{\underline{i}} = -\omega\underline{j}$ and $\dot{\underline{j}} = \omega\underline{i}$.

Substituting in (A-2)

$$-V\underline{j} = \dot{\Lambda}\underline{i} - \omega(R+\Lambda)\underline{j} + \dot{L}\underline{j} + \omega L\underline{i} \qquad \text{(A-3)}$$

Equating components in (A-3)

$$\dot{\Lambda} = -\omega L \qquad \text{(A-4)}$$

$$\dot{L} = -V + \omega(R+\Lambda) \qquad \text{(A-5)}$$

The above equations are (1) and (2) in Section III.

For a horizontal turn we have from Figure 14

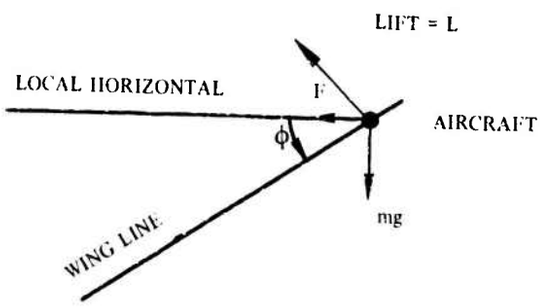

Figure 14: Horizontal Turn

L cos φ = mg, and Horizontal Force=F=L sin φ.

Now for a coordinated turn

$F = m\omega^2 r = m\omega V$ since $V = \omega R$.

By eliminating F and L from our equations

$m\omega V = mg \tan \varphi$

and solving for ω

$$\omega = \frac{g}{V} \tan \varphi \qquad \text{(A-6)}$$

The preceding equation is (3) of Section III.

APPENDIX B

Stability Analysis of the $\dot{\Delta}$ and $\dot{L}$ Equations

The stability analysis will be done for the $\dot{x}_1$ and $\dot{x}_2$, equations (9) and (10). They are directly proportional to $\dot{\Delta}$ and $\dot{L}$ since $\dot{x}_1 = \frac{\dot{\Delta}}{R}$ and $\dot{x}_2 = \dot{L}/R$.

An equilibrium point ($\dot{x}_1 = \dot{x}_2 = 0$) for (9) and (10) is given by $x_1 = x_2 = 0$ which means $L = \Delta = 0$ also since $x_1 = \Delta/R$ and $x_2 = L/R$. The fact that (10) is zero is true from (3) since $\omega V = g \tan \varphi$ or, equivalently, $\frac{V^2}{R} = g \tan \varphi$. The stability of this equilibrium point can be determined by linearizing equations (9) and (10) and then letting $x_1 = x_2 = 0$ giving:

$$\delta\dot{x}_1 = -g/V \tan(.524)\ \delta x_2 \qquad \text{(B-1)}$$

$$\delta\dot{x}_2 = \frac{g}{V}\tan(.524)\,\delta x_1 - \frac{g}{V}(K_1R\delta x_1 + K_2R\delta x_2)\sec^2(.524) \qquad \text{(B-2)}$$

Using the values of the simulation, V = 300 fps, R = 4844 ft, and the definitions $c_1 = K_1R$ and $c_2 = K_2R$, the above equations can be written in vector form as

$$\begin{pmatrix} \delta\dot{x}_1 \\ \delta\dot{x}_2 \end{pmatrix} = \begin{bmatrix} 0 & -.0622 \\ .1435c_1 + .0622 & .1435c_2 \end{bmatrix} \begin{pmatrix} \delta x_1 \\ \delta x_2 \end{pmatrix} \qquad \text{(B-3)}$$

Local stability is now dependent on the eigenvalues of the matrix in (B-3). Using (B-3), these eigenvalues, λ, can be determined from the following equation:

$$\lambda^2 - .1435c_2\lambda + .0089c_1 + .0039 = 0 \qquad \text{(B-4)}$$

Equation (B-4) will have roots with negative real parts, which guarantees a stable equilibrium point, if $c_1 > 0$ and $C_2 < 0$. Thus, we must also have that $K_1 > 0$ and $K_2 < 0$.

From the simulation study the values of c_1 and c_2 were determined as 1.7 and -1.7, respectively. A second order system has a characteristic equation of the general form

$$\lambda^2 + 2\zeta\omega_n\lambda + \omega_n^2 = 0 \qquad \text{(B-5)}$$

where ω_n is the natural frequency and ζ is the damping ratio. Substituting the values of c_1 and c_2 into (B-4) and solving for ω_n and ζ:

$$\omega_n = .137 \text{ rad/sec} \qquad \text{(B-6)}$$

$$\zeta = 0.89 \qquad \text{(B-7)}$$

If $|c_1| > |c_2|$ the system tends to become more oscillatory but has a faster response. By limiting L as in the simulation at large distances from the circular path, the system has essentially reduced the effect of c_2L and thus $|c_1|$ is <u>effectively</u> larger than $|c_2|$ giving the faster response. However, in the simulation $|c_1| = |c_2|$ after L is no longer limited (near the circular flight path), the system has the desirable damping ratio given by (B-7).

Finally a plot of $x_1 = \Delta/R$ and $x_2 = L/R$ is given in Figure 15 (page 31). This plot is for the simulated system as given in Figure 4, and, therefore, <u>includes</u> the <u>limiters</u> and the <u>time lag</u> of two seconds. The direction of motion is shown by the arrows. The stable equilibrium point is clearly evident at $\Delta/R = L/R = 0$. An unstable equilibrium point is evident at $\Delta/R \approx -1.8$ and $L/R = 0$. This second equilibrium point can also be solved for by equating $\dot{x}_1 = \dot{x}_2 = 0$ and looking for a second solution. Notice that the local stability analysis of this section only applies approximately to Figure 15 since the stability analysis did not include the limiters or the time delay. However, we see that the local stability analysis correctly predicted the stable equilibrium point at the origin.

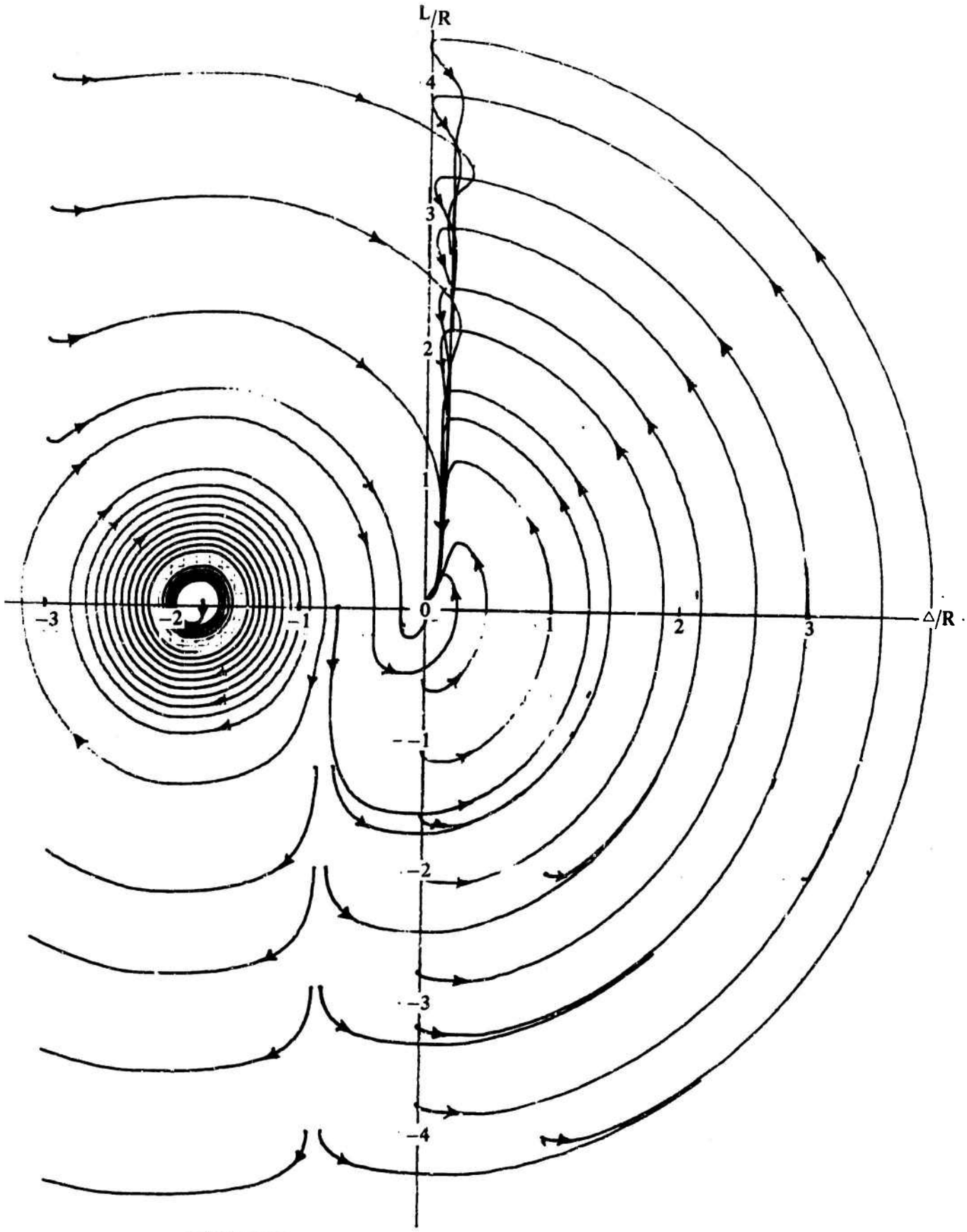

Figure 15: Δ/R vs. L/R for the Simulated System.

Figure 15 shows that as long as the approach guidance is activated with $\Delta/R > -0.7$, when the target is more than 0.3R ft. off the left wing, then the system behaves well. Normally the target will be detected only under these conditions, so this represents no real restriction for present systems.

For future systems, where target positions can be approached from any point, the approach guidance should not be activated in approximately a circular region of radius 1.1R with center at $\Delta = -1.8R$ and $L = 0$.

APPENDIX C

Analog Simulation

The analog simulation begins by programming equations (9), (10), and (11). Choose a velocity of 300 fps, and solve for R from (3) where $V = \omega r$,

$$R = \frac{V^2}{g \tan (.524)} = 4844 \text{ ft.} \qquad \text{(C-1)}$$

The angle φ has been defined as

$$\varphi = .524 + \delta\varphi$$

and we define

$$c_1 = K_1 R \text{ and } c_2 = K_2 R \qquad \text{(C-2)}$$

Equations (9), (10) and (11) now become:

$$\dot{x}_1 = -.1073 x_2 \tan \varphi \qquad \text{(C-3)}$$

$$\dot{x}_2 = -.06195 + .1073 \tan \varphi + .1073 x_1 \tan \varphi \qquad \text{(C-4)}$$

$$\delta\varphi = c_1 x_1 + c_2 x_2 \qquad \text{(C-5)}$$

Equations for computer solution are magnitude scaled using:

$$x_{1N} = 10 \qquad \dot{x}_{1N} = 2$$

$$x_{2N} = 10 \qquad \dot{x}_{2N} = 2$$

Our resulting equations are

$$\dot{x}_{1N} \left(\frac{\dot{x}_1}{\dot{x}_{1N}} \right) = -.1073 x_{2N} \left(\frac{x_2}{x_{2N}} \right) \tan \varphi$$

$$\dot{x}_{2N} \left(\frac{\dot{x}_2}{\dot{x}_{2N}} \right) = -.06195 + .1073 \tan \varphi + .1073 x_{1N} \left(\frac{x_1}{x_{1N}} \right) \tan \varphi$$

Letting

$$z_1 = \frac{x_1}{x_{1N}} \qquad z_2 = \frac{x_2}{x_{2N}}$$

$$\dot{z}_1 = \frac{\dot{x}_1}{x_{1N}} \qquad \dot{z}_2 = \frac{\dot{x}_2}{x_{2N}}$$

We have:

$$2\dot{z}_1 = -.1073\ (10)\ z_2 \tan \varphi$$

$$2\dot{z}_2 = -.06195 + .1073 \tan \varphi + .1073\ (10) \tan \varphi$$

Our programmed equations are:

$$\dot{z}_1 = -.5365\ z_2 \tan \varphi \qquad \text{(C-6)}$$

$$\dot{z}_2 = -.03097 + .05365 \tan \varphi + .5365\ z_1 \tan \varphi \qquad \text{(C-7)}$$

$$\delta\varphi = 10C_1Z_1 + 10C_2Z_2 \qquad \text{(C-8)}$$

Therefore potentiometers preceding the integrators are set at $\frac{\dot{x}}{x} = \frac{2}{10} = .2$

NOTE: The computer is then time scaled by a factor of 5; the computer solution is speeded up 5 times by multiplying the input to all integrators by 5. Then the limiters and time lag are added; time scale the latter by a factor of 5. A computer flow diagram of the simulation is shown in Figure 16.

The ground trace was programmed from the following equations derived with the aid of Figure 17. Ground coordinates are x and y. The moving coordinates are "a" and "b" as seen by a target observer and defined along $\underline{1}_\setminus$ and $\underline{1}_\perp$. From Figure 17 we have:

$$x = -a \cos \theta - b \sin \theta \qquad \text{(C-9)}$$

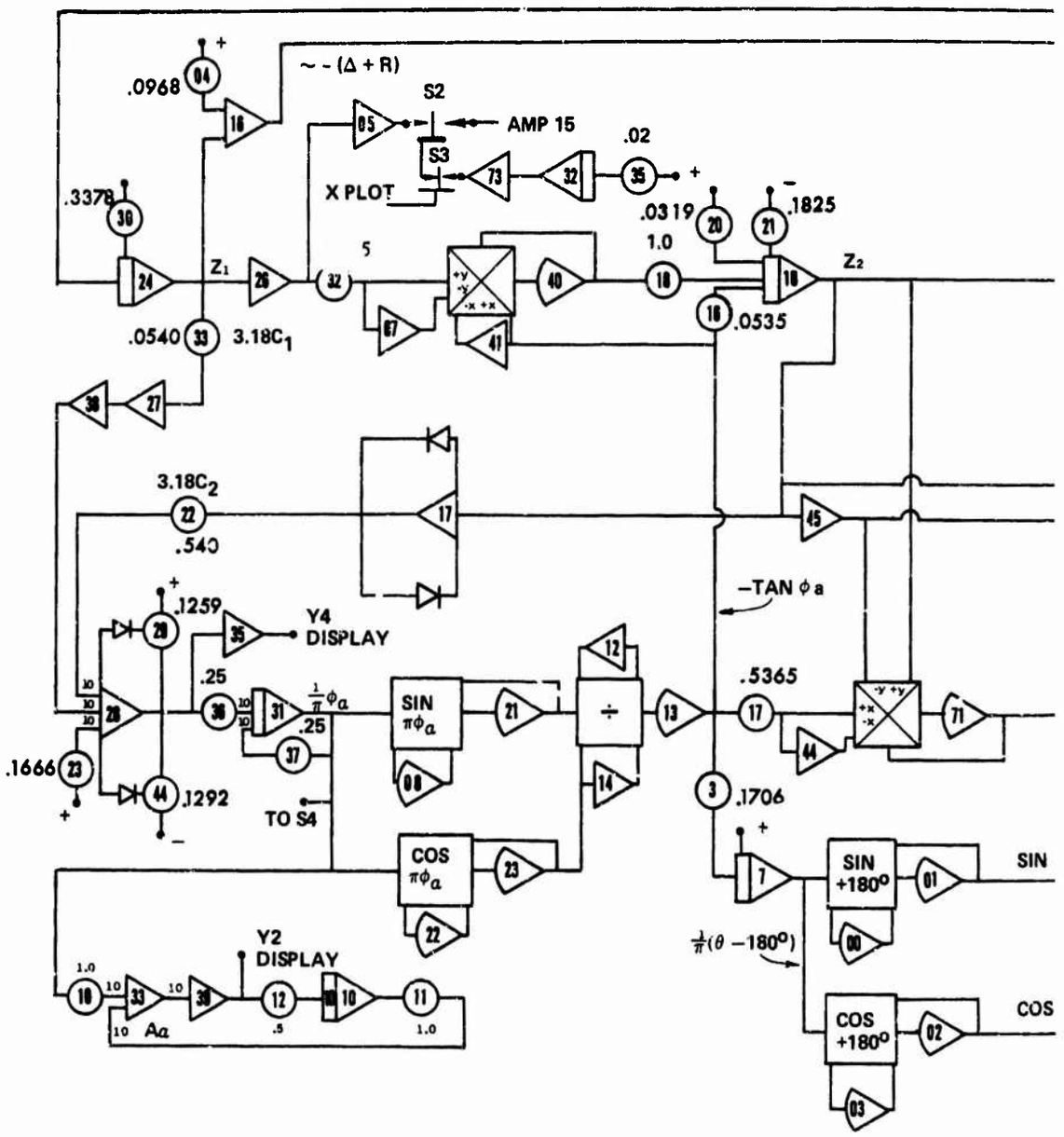

FIGURE 16 – COMPUTER FL

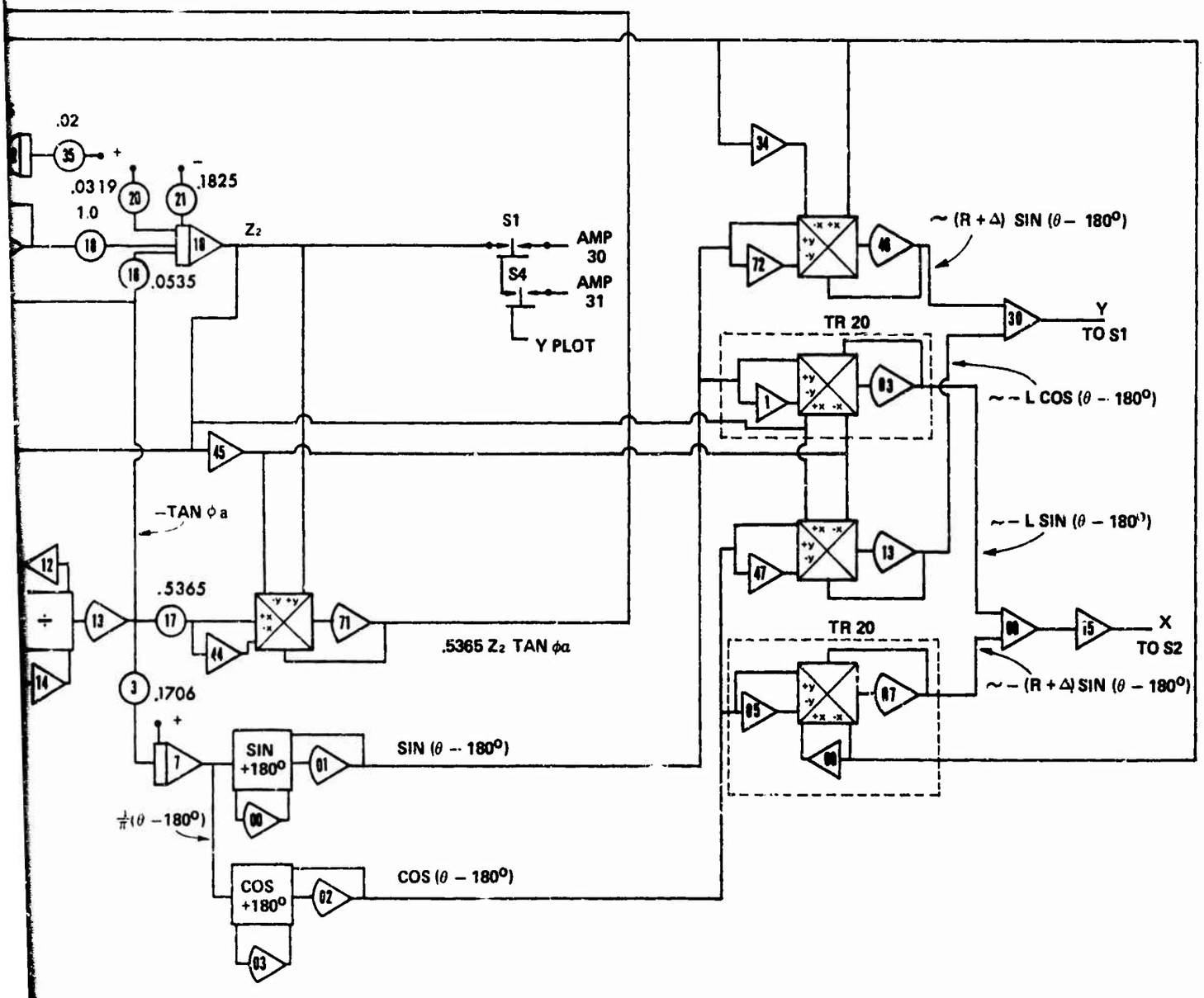

FIGURE 16 – COMPUTER FLOW DIAGRAM

B

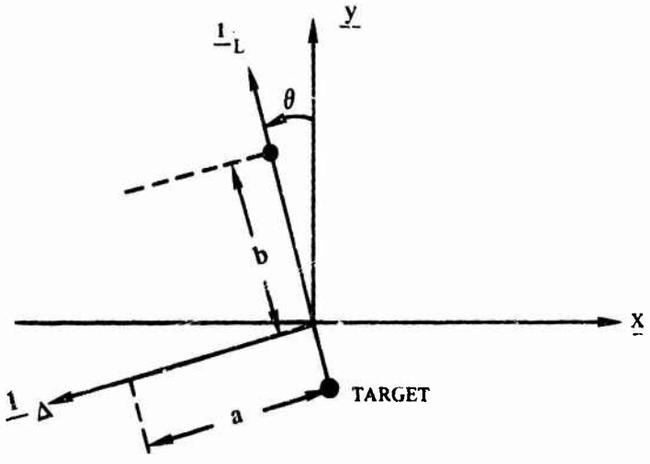

Figure 17: Relationship Between Ground Coordinates (x – y) and the Moving Coordinates (Δ – L)

$$y = b \cos \theta - a \sin \theta \qquad \text{(C-10)}$$

However, a target observer sees the negative of what an aircraft observer would see; therefore,

$$a = -(\Delta+R) \qquad \text{(C-11)}$$

$$b = -L \qquad \text{(C-12)}$$

[See Figure 13.]

Substituting (C-11) and (C-12) into (C-9) and (C-10):

$$x = (\Delta+R) \cos \theta + L \sin \theta \qquad \text{(C-13)}$$

$$y = -L \cos \theta + (\Delta+R) \sin \theta \qquad \text{(C-14)}$$

However, since the angle θ will overload on the computer if $|\theta| > 180^{\circ}$, the following equations were actually programmed:

$$x = -(\Delta+R)\cos(\theta-180^{o})-L \sin (\theta-180^{o}) \qquad (C\text{-}15)$$

$$y = L \cos(\theta-180^{o})-(\Delta+R)\sin(\theta-180^{o}) \qquad (C\text{-}16)$$

Equations (C-15) and (C-16) are identical to (C-13) and (C-14) since sin $(\theta-180^{o}) = -\sin\theta$, and cos $(\theta-180^{o}) = -\cos\theta$. The angle θ was generated by integrating ω; i.e.,

$$\theta = \int_{o}^{t} \omega dt = \int_{o}^{t} \left(\frac{g \tan \varphi_a}{V}\right) dt$$

Finally after many runs to obtain a satisfactory response, the values of K_1 and K_2 were calculated from (C-2)

$$K_1 = \frac{c_1}{R} = 3.5 \times 10^{-4} \text{ rad/ft}$$

$$K_2 = \frac{c_2}{R} = -3.5 \times 10^{-4} \text{ rad/ft}$$

The results of the simulation are given graphically in Figures 5 through 10.

Unclassified

Security Classification

DOCUMENT CONTROL DATA - R & D

(Security classification of title, body of abstract and indexing annotation must be entered when the overall report is classified)

1. ORIGINATING ACTIVITY (Corporate author)	2a. REPORT SECURITY CLASSIFICATION
Hq USAFA (Directorate of Faculty Research) USAF Academy, Colorado 80840	Unclassified
	2b. GROUP

3. REPORT TITLE

AN APPROACH GUIDANCE SYSTEM FOR SIDE-FIRING TACTICAL AIRCRAFT

4. DESCRIPTIVE NOTES (Type of report and inclusive dates)

Technical Report

5. AUTHOR(S) (First name, middle initial, last name)

Lt Colonel Bradford W. Parkinson
Major Edward J. Bauman
Captain Jack C. Henry

6. REPORT DATE	7a. TOTAL NO. OF PAGES	7b. NO. OF REFS
October 1970		

8a. CONTRACT OR GRANT NO.	9a. ORIGINATOR'S REPORT NUMBER(S)
b. PROJECT NO.	TR 70-4
c.	9b. OTHER REPORT NO(S) (Any other numbers that may be assigned this report)
d.	None

10. DISTRIBUTION STATEMENT

Distribution of this document is unlimited

11. SUPPLEMENTARY NOTES	12. SPONSORING MILITARY ACTIVITY
	Directorate of Faculty Research (DFSFR) USAF Academy, Colorado 80840

13. ABSTRACT

The present approach guidance scheme is one of controlling the aircraft's velocity vector; however, this scheme has two major disadvantages:

(1) It's a difficult flying task for the pilot, and
(2) When the aircraft arrives tangent to the circular path, a violent maneuver is usually required to achieve the proper bank angle to stay on the desired circular path.

An improved method for controlling the side firing AC-130 and AC-119 into circular attack geometry eliminates these disadvantages. Furthermore, with this improved system the bank angle rates never exceed 3 or 4 degrees per second. This control scheme was simulated on the analog computer and the results are presented graphically. The simulation showed that the bank angle, command-control scheme is effective for distances out to five circular orbit radii from the target and is effective for all aircraft headings (with one exception which is discussed in a stability study in the appendix). The initial test flight showed that the bank angle control scheme behaved very well, and its overall performance was near that predicted. Relatively minor modifications can incorporate this control scheme into existing analog computers on board the aircraft.

DD FORM 1 NOV 65 1473

Unclassified

Security Classification

14 KEY WORDS	LINK A		LINK B		LINK C	
	ROLE	WT	ROLE	WT	ROLE	WT
approach guidance scheme bank angle command control scheme circular attack geometry approach guidance scheme AC-130 bank angle command control scheme						